

A genome-wide screen in *Escherichia coli* reveals that ubiquinone is a key antioxidant for metabolism of long chain fatty acids

Shashank Agrawal^{1#}, Kanchan Jaswal^{1#}, Anthony L Shiver², Himanshi Balecha¹, Tapas Patra^{1†} and Rachna Chaba^{1*}

¹Department of Biological Sciences, Indian Institute of Science Education and Research (IISER) Mohali, SAS Nagar, Punjab 140306, India; ²Department of Bioengineering, Stanford University, Stanford, California 94305, USA

Running title: Role of ubiquinone in LCFA metabolism

[#]S.A. and K.J. contributed equally to this work.

*To whom correspondence should be addressed:

Rachna Chaba, Department of Biological Sciences, Indian Institute of Science Education and Research (IISER) Mohali, SAS Nagar, Punjab 140306, India.

Email: rachnachaba@iisermohali.ac.in; rachnachaba@gmail.com

Keywords: fatty acid metabolism, long chain fatty acids, respiratory chain, electron transport, quinone, oxidative stress, non-fermentable carbon sources, *ubiI*, *ubiK*, bacterial genetics

ABSTRACT

Long chain fatty acids (LCFAs) are used as a rich source of metabolic energy by several bacteria including important pathogens. Since LCFAs also induce oxidative stress, which may be detrimental to bacterial growth, it is imperative to understand the strategies employed by bacteria to counteract such stresses. Here, we performed a genetic screen in *Escherichia coli* on the LCFA, oleate, and compared our results with published genome-wide screens of multiple non-fermentable carbon sources. This large-scale analysis revealed that amongst components of the aerobic electron transport chain (ETC), only genes involved in the biosynthesis of ubiquinone, an electron carrier in the ETC, are highly required for growth in LCFAs when compared to other carbon sources. Using genetic and biochemical approaches, we show that this increased requirement of ubiquinone is to mitigate elevated levels of reactive oxygen species (ROS) generated by LCFA degradation. Intriguingly, we find that unlike other ETC components whose requirement for growth is inversely correlated with the energy yield of non-fermentable carbon sources, the requirement of

ubiquinone correlates with oxidative stress. Our results therefore suggest that a mechanism in addition to the known electron carrier function of ubiquinone is required to explain its antioxidant role in LCFA metabolism. Importantly, among the various oxidative stress combat players in *E. coli*, ubiquinone acts as the cell's first line of defense against LCFA-induced oxidative stress. Taken together, our results emphasize that ubiquinone is a key antioxidant during LCFA metabolism and therefore provides a rationale for investigating its role in LCFA-utilizing pathogenic bacteria.

INTRODUCTION

Long chain fatty acids (LCFAs) are carboxylic acids with an unbranched aliphatic chain of 12-20 carbon atoms. Several bacterial pathogens such as *Mycobacterium tuberculosis*, *Pseudomonas aeruginosa*, and *Salmonella typhimurium* metabolize LCFAs derived from host tissues, which enable their survival in harsh environments and contribute to their virulence (1-3). Much of our understanding of LCFA metabolism is obtained from studies in *E. coli*. LCFA metabolism is mediated by proteins

encoded by the *fad* (fatty acid degradation) genes that transport LCFAs inside the cell and subsequently degrade it to acetyl-CoA via the β -oxidation pathway. Acetyl-CoA feeds into the tricarboxylic acid (TCA) and glyoxylate cycles to generate metabolic intermediates for growth. Reduced cofactors generated during β -oxidation and TCA cycle are oxidized by the electron transport chain (ETC) resulting in production of ATP. The *fad* genes are controlled at a transcriptional level by three regulatory systems: i) positive regulation by the global cyclic AMP receptor protein-cyclic AMP complex (catabolite repression), ii) negative regulation by the transcriptional regulator, FadR, repression of which is relieved by binding to acyl-CoA, a metabolic intermediate in LCFA degradation, and iii) negative regulation by the ArcA-ArcB two-component system [reviewed in (4,5)].

Growth on LCFAs requires the presence of either oxygen as terminal electron acceptor (aerobic metabolism) or alternative electron acceptor such as nitrate (anaerobic metabolism). Thus, LCFAs are non-fermentable carbon sources, which unlike glucose, a fermentable carbon source, require optimal functioning of ETC (6,7). Components of ETC are located in the inner membrane of *E. coli*. During aerobic metabolism NADH and FADH₂ are oxidized by NADH dehydrogenases (Ndh and Nuo) and succinate dehydrogenase (Sdh), respectively, and the electrons are transferred to the lipid-soluble electron carrier, ubiquinone. The reduced form of ubiquinone, ubiquinol, in turn donates electrons to the terminal oxidases, cytochrome *bo* (Cyo) and cytochrome *bd* (Cyd), which further transfer electrons to molecular oxygen reducing it to water molecule. During the flow of electrons through ETC, Nuo, Cyo and Cyd generate proton motive force that further drives ATP synthesis through ATP synthase (8,9). Consistent with the increased requirement of ETC on non-fermentable carbon sources, in contrast to growth on glucose, mutants of several ETC components exhibit severe growth defect on succinate, acetate, lactate and malate (9-12). However, the importance of ETC components for growth on LCFAs has not been examined. Different non-fermentable carbon sources enter into the TCA cycle at varied steps and are theoretically expected to generate different amount of reduced cofactors, thus even amongst these

carbon sources there could be a difference in the requirement of ETC components. Hence, the requirement of individual components of the ETC in LCFA metabolism should be investigated.

In addition, a recent study has shown that LCFAs induce oxidative stress in *E. coli* (13), however, the mechanism by which bacteria combat this stress is not known. The enzymatic scavengers (peroxidases, catalases and superoxide dismutases) are known to be the major oxidative stress combat players in bacteria (14). On the other hand, the role of the ETC component, ubiquinone, as an antioxidant in bacteria is underappreciated. There is only one report in *E. coli* that suggested ubiquinone to function as an antioxidant based on oxidative stress phenotypes of mutants defective in ubiquinone biosynthesis (15). But, how ubiquinone counteracts ROS, what is the physiological condition under which ubiquinone plays a predominant role, and what is the relative contribution of ubiquinone to the overall oxidative stress response remains to be assessed. The remarkable use of LCFAs by pathogens such as *Mycobacterium tuberculosis*, *Pseudomonas aeruginosa*, and *Salmonella typhimurium* (1-3) warrants a detailed investigation of the strategies employed by bacteria to mitigate LCFA-mediated oxidative stress.

With the motive to fill in the above-mentioned knowledge gaps in LCFA metabolism, using the Keio deletion library of *E. coli* (16), we performed a quantitative genetic screen on oleate (C18:1 cis-9) and compared our LCFA dataset with recent high-throughput genetic screens of additional carbon sources (17). This comparative analysis revealed that amongst all aerobic ETC components only genes involved in the biosynthesis of ubiquinone are more important for growth in LCFAs when compared to other non-fermentable carbon sources. Our detailed studies show that of the various oxidative stress combat players in *E. coli*, ubiquinone is the key player that mitigates elevated levels of ROS generated by LCFA degradation, however, its role as an antioxidant cannot be described solely by its known electron carrier function in the ETC.

RESULTS

A chemical-genomic screen reveals the pathways used by *E. coli* to aerobically metabolize long chain fatty acids

We tested the ability of 3994 mutants from the Keio deletion library to grow on oleate as the sole carbon source. To measure fitness defects during growth on oleate, we pinned the Keio library onto M9 minimal agar plates containing either oleate or glucose as the sole carbon source. Since oleate was solubilized in the detergent Brij-58, the growth medium containing glucose was also supplemented with Brij-58. We took images of the plates at a single time point and quantified colony size using image analysis software (18). Replicate colony size measurements were reproducible in the screen (Fig. 1A, $R=0.86$). We then assigned a fitness-score to mutants in the oleate condition by calculating the statistical significance of the difference in colony size between oleate and the glucose control using an established analysis pipeline (19) with slight modifications (Experimental Procedures). To facilitate the comparison of oleate to other carbon sources, we reanalyzed data from a previous screen (17), comparing both fermentable (glucosamine, N-acetyl glucosamine and maltose) and non-fermentable (acetate, succinate and glycerol) carbon sources to glucose as a control. The fitness-scores we report thus represent the statistical significance of a change in colony size on a particular carbon source as compared to growth on glucose with positive and negative fitness-scores representing increased and decreased colony size, respectively. A full list of fitness scores of Keio library strains in different carbon sources (normalized to a glucose control) is available in Dataset S1A.

The screen identified a large number of mutants with severe growth defects on oleate. To better understand the physiological basis for these growth defects, we performed a global analysis using Gene Set Enrichment Analysis (GSEA) and gold-standard biological pathways (20-22), to find pathways that play a significant role in growth on oleate (Dataset S1B). Importantly, global analysis highlighted the β -oxidation pathway (FDR q-value: 1.1%), critical for the utilization of LCFAs as an energy source, as a unique signature of growth on oleate. This result emphasizes the robustness of our high-throughput genetic screen and of our statistical approach. In addition, oleate, acetate and succinate shared a significant enrichment in the TCA and glyoxylate cycles (FDR q-value $<5\%$), a result consistent with these

pathways being critical for generation of reduced cofactors and metabolites for growth on non-fermentable carbon sources (4,5). Furthermore, oleate, acetate and succinate utilization exhibited enrichment in multiple pathways for electron transfer activity (FDR q-value $<5\%$), underscoring the importance of ETC for energy generation during growth on non-fermentable carbon sources. We also performed GSEA analysis for protein complexes with 3 or more proteins (20,22). Oleate, acetate and succinate utilization were enriched for ETC complexes, NADH dehydrogenase I (Nuo) (FDR q-value $<1\%$) and succinate dehydrogenase (FDR q-value $<7\%$) (Dataset S1C). The enriched metabolic pathways and complexes for oleate utilization are depicted in Fig. 1B.

Although glycerol is considered to be a non-fermentable carbon source, this substrate did not show a significant enrichment of any of the ETC pathways or complexes in our GSEA analysis. We speculate that since there is ATP generation (by substrate-level phosphorylation) after the entry of glycerol in the later part of glycolysis (23), this ATP might allow for growth on glycerol. Moreover, the fermentative utilization of glycerol has also been suggested (24). Thus, for detailed studies on the requirement of ETC components we further focused on oleate, acetate and succinate. To circumvent problems of high-throughput screens (incorrect strains, suppressors and cross-contamination), before a detailed follow-up analysis of ETC mutants, we verified phenotypes using transductants. Further, since oxygen availability to cells in a colony varies with the size of colony (25), in our subsequent experiments we also validated the requirement of ETC components in aerobic metabolism by assessing their phenotypes in liquid medium.

Requirement of ubiquinone does not correlate with the energy yield of non-fermentable carbon sources

A comparison of our LCFA dataset with GSEA analysis for additional carbon sources clearly showed that ETC is critical for growth of *E. coli* on non-fermentable carbon sources. However, there was a difference in the requirement of various ETC components. Of the two NADH dehydrogenases involved in ETC, Ndh is known to be more important during aerobic respiration whereas Nuo is essential for dimethyl sulfoxide

and fumarate (anaerobic) respiration (26,27). However, we noted that for aerobic metabolism of oleate, acetate, and succinate, Nuo was important whereas Ndh was dispensable (Fig. 1C). Early studies had reported the growth defect of *nuo* mutants in acetate, however they did not assess the relative requirement of Ndh and Nuo (10,28). We validated our results by comparing the growth profile of Δnuo (the entire *nuo* operon is deleted) and Δndh in liquid medium; only Δnuo showed significant growth defect in oleate, acetate, and succinate (Fig. 2). We suggest that since Nuo couples NADH oxidation to proton translocation ($H^+/e^- = 2$) whereas Ndh does not ($H^+/e^- = 0$) (8,26), it is likely that growth on non-fermentable carbon sources is dependent on Nuo for ATP production. Further, amongst oleate, acetate, and succinate, Nuo was more significantly required for growth in acetate (Fig. 1C and 2) that has the worst net ATP yield of these three carbon sources (4). Whereas Δnuo did not grow in acetate, the strain exhibited an extended lag in oleate and succinate, and then grew at the same rate and to the same yield as wild-type (WT) (Fig. 2). To rule out the possibility that Δnuo strain was picking up suppressors in oleate and succinate, we sub-cultured cells from stationary phase. We again observed extended lag in succinate and oleate. Similar to Nuo, Cyo which is the major terminal oxidase during aerobic metabolism and also generates proton motive force in the ETC ($H^+/e^- = 2$) (8), was maximally required in acetate (Fig. 1C). Collectively, our results suggest that the quantitative contribution of Nuo and Cyo to growth on non-fermentable carbon sources is inversely correlated with the energy yield of these substrates.

In contrast to Nuo and Cyo, we observed that the requirement of ubiquinone was more in oleate compared to other non-fermentable carbon sources (Fig. 1C). In *E. coli*, the biosynthesis of ubiquinone is known to involve at least twelve *ubi* genes (9,29) (Fig. 1B). The data for only seven *ubi* deletion strains were available from previous genetic screens for comparison with our oleate dataset (17) (Fig. 1C). In independent studies the growth phenotype of null mutants of five *ubi* genes (*ubiE*, *ubiF*, *ubiH*, *ubiI* and *ubiX*) have been reported in succinate (30-33). In our analysis, only the phenotype of *ubiF*, *ubiH* and *ubiI* mutants agreed with their known phenotypes in succinate

(30,31) (Fig. 1C). We thus constructed several transductants of all five *ubi* mutants and assessed their growth at a candidate level (Fig. S1). The phenotype of all *ubi* mutants corroborated with their known phenotype in succinate: *ubiE*, *ubiF* and *ubiH* mutants exhibited no growth (30,32), *ubiX* mutant showed growth defect (33) and *ubiI* mutant displayed wild-type growth (30,31). In acetate, all *ubi* mutants had a phenotype similar to that in succinate. In oleate, *ubi* mutants either did not grow at all (*ubiE*, *ubiF* and *ubiH*) or showed significant growth defect (*ubiI* and *ubiX*) (Fig. S1). Upon relating the growth profile of *ubi* deletion strains observed in our study with their ubiquinone levels reported in the literature we find that mutants with no detectable ubiquinone (*ubiE*, *ubiF* and *ubiH*) (30,32) do not grow in any of the three non-fermentable carbon sources, whereas a *ubiI* mutant which produces reduced levels of ubiquinone (30,31) exhibits growth defect only in oleate. UbiI catalyzes C5-hydroxylation of the 3-octaprenylphenol intermediate in the ubiquinone biosynthesis pathway and the residual level of ubiquinone in a $\Delta ubiI$ strain is attributed to the suboptimal C5-hydroxylase activity of a C6-monooxygenase, UbiF (31).

For the last several decades, the increased requirement of ubiquinone for energy generation during growth with succinate compared to glucose has been the rationale for identifying genes involved in ubiquinone biosynthesis (34,35). Despite this, it was surprising that a recent study showed that $\Delta ubiI$, where ubiquinone level is reduced to only ~10-15% of WT level, exhibited normal growth in succinate (30,31). Data from genetic screens and candidate studies in solid media reinforce that even ~10-15% ubiquinone is sufficient for growth in succinate, whereas, this ubiquinone level is suboptimal for growth in LCFAs.

We investigated further the differential requirement of ubiquinone on non-fermentable carbon sources. We compared the growth profile of $\Delta ubiH$ and $\Delta ubiI$ strains in liquid media. Whereas $\Delta ubiH$ showed a growth reduction on glucose, the strain did not grow at all with oleate, acetate and succinate (Fig. 3A). On the other hand, $\Delta ubiI$ showed a significant growth defect only in oleate (Fig. 3A); the growth defect was complemented by *ubiI* cloned on plasmid (Fig.

S2). Taken together, our analysis of the growth phenotypes of ETC mutants on various carbon sources highlights a specific role of ubiquinone in LCFA metabolism.

Ubiquinone is maximally required in oleate to mitigate elevated levels of ROS

E. coli grown in oleate is reported to accumulate higher levels of ROS compared to cultures grown in glucose (13). In a separate study, ubiquinone was suggested to function as an antioxidant in *E. coli* (15). A *ubiCA* knockout which produces no detectable ubiquinone (36) was shown to exhibit several oxidative stress phenotypes in LB: accumulation of superoxide and H₂O₂ in membranes, hypersensitivity to oxidative stress inducing agents, and upregulation of catalase (15). In the present work, whereas *ubi* deletion strains that produce no detectable ubiquinone did not grow at all in oleate, acetate and succinate, *ubil* mutant that produces decreased levels of ubiquinone showed significant growth defect only in oleate (Fig. 1C and 3A; Fig. S1). Collectively, these observations led us to argue that of the above three non-fermentable carbon sources, *E. coli* generates highest ROS levels when cultured in oleate and the increased requirement of ubiquinone in oleate is to counteract elevated levels of ROS.

Consistent with the above proposal, glutathione and thiourea, widely used chemical antioxidants in *E. coli* (37-39), partially recovered the growth defect of *Δubil* in oleate (Fig. 3B and C). We did not observe a complete recovery since another factor responsible for the poor growth of *Δubil* in oleate would be reduced energy generation due to lowering of ETC function. Interestingly, WT strain also grew better in the presence of glutathione and thiourea consistent with previous report that cells suffer oxidative stress during growth in oleate (13) (Fig. 3B and C). Further, we tested whether *E. coli* indeed generates highest ROS levels when cultured in oleate in comparison to acetate and succinate. For this, we measured intracellular ROS levels in WT and *Δubil* cultured in Tryptone Broth (TB) supplemented with various carbon sources by a colorimetric assay based on the reduction of nitroblue tetrazolium (NBT) dye by superoxide. WT had highest ROS levels in TB-Ole; ~1.5-fold higher than basal medium (Fig. 3D). This fold

change was comparable with a previous report where ~2-fold higher ROS levels were observed in WT cells grown in minimal medium supplemented with oleate compared to cells grown in glucose supplemented medium (13). Moreover, ROS levels further increased in *Δubil* in all media conditions with maximal ROS levels again in TB-Ole grown cells (Fig. 3D). Brij-58 alone did not result in increased ROS. Importantly, when ubiquinone-8 was supplied exogenously, ROS levels decreased by ~15-25% in WT grown in TB-Ole and *Δubil* grown either in TB or TB-Ole (Fig. 3E), reiterating that ubiquinone relieves oxidative stress.

NBT enters inside the cells and has been extensively used in *E. coli* and other gram-negative bacteria to measure intracellular superoxide (40-43). We independently validated that the reduction of NBT reports on intracellular superoxide levels by showing that overexpressing superoxide dismutase, SodA, from plasmid decreases NBT signal in all tested media conditions (TB, TB-Brij and TB-Ole; Fig. S3A and B). We further confirmed our results from NBT assay by using a fluorescent dye, dihydroethidium (DHE) that also detects superoxide (Fig. S3C) (44). Experiments involving measurement of ROS levels were carried out in TB to support the growth of *ubil* knockout, which shows growth defect in minimal medium containing oleate as the sole carbon source (Fig. S1; Fig. 3A). Furthermore, since TB causes mild catabolite repression (45), supplemented carbon sources are expected to be co-utilized with carbon components of TB. As a representative, the increase in biomass and transcript levels of *fadL* (outer membrane transporter for LCFAs) and *fadE* (acyl-CoA dehydrogenase involved in β-oxidation of LCFAs) in WT grown in TB-Ole confirmed the co-utilization of oleate with TB (46,47) (Fig. S4A and B). Since maximum difference in ROS levels was observed in the stationary phase (time point T4 in Fig. S4A) (Fig. S4C), for single time point experiments cultures were sampled in this growth phase.

Ubiquinone is a major antioxidant during oleate metabolism

We tested whether in addition to ubiquinone other oxidative stress response players counteract ROS generated by oleate. In TB medium, ROS levels

were ~1.3 to 1.7 fold higher when strains lacked either the *ubi* genes or other players [(alkyl hydroperoxide reductase subunit- AhpC, oxidative stress regulator- SoxR, superoxide dismutase- SodA, catalase- KatE, and an enzyme involved in glutathione biosynthesis, GshB) (14,15)] (Fig. 4A). In contrast, in TB-Ole medium, ROS levels increased only in *ubi* deletion strains (Fig. 4A). We considered two possibilities for the TB-Ole results: *i*) there is redundancy of enzymatic scavengers and their regulators, and *ii*) as long as ubiquinone is present, it does not allow ROS to build-up further in TB-Ole thereby reducing dependency on other players. Consistent with the second possibility, the enzymatic scavengers, *katG* and *ahpC* were induced (~2-fold) by oleate only in a $\Delta ubiI$ strain (Fig. 4B and C), and this increased expression was reduced by ~25% upon exogenous supplementation of ubiquinone-8 (Fig. 4D).

Our above data suggests that ubiquinone is a major player that mitigates LCFA-mediated oxidative stress. We examined whether this defense system is induced by LCFAs. *E. coli* ubiquinone is designated as Q₈ and exists in two redox states in the cell, ubiquinone and ubiquinol (9). We extracted lipids from WT and several *fad* knockouts, separated lipids by HPLC, and measured total Q₈ content (ubiquinone and ubiquinol). Peaks for ubiquinone and ubiquinol in the samples were assigned based on the elution time of pure standards, and the reduction of ubiquinone and ubiquinol peaks in $\Delta ubiI$ (Fig. S5). In WT cells, Q₈ content was ~1.8-fold higher in TB-Ole compared to TB (Fig. 4E). Q₈ levels did not increase in cells grown in TB-Brij. Importantly, the increase in Q₈ levels was dependent on oleate utilization since Q₈ levels did not increase in TB-Ole in *fad* mutants defective in LCFA transport and β -oxidation ($\Delta fadL$, $\Delta fadD$ and $\Delta fadE$) (Fig. 4E). Interestingly, the increase in ROS levels in TB-Ole was also due to oleate utilization; compared to TB, ROS level did not exhibit considerable increase in TB-Ole in *fad* mutants (Fig. 4F). ROS level in TB was higher in $\Delta fadD$ strain possibly due to accumulation of endogenous free fatty acids (48,49).

$\Delta ubiI\Delta ubiK$ double mutant produces no detectable ubiquinone

While this manuscript was under preparation, an uncharacterized gene, *yqiC* (renamed as *ubiK*), was identified as a ubiquinone biosynthesis player based on the reduction of ubiquinone levels to ~20% of WT in $\Delta ubiK$ strain (29), however, the growth of $\Delta ubiK$ strain on non-fermentable carbon sources has not been evaluated. Importantly, in our comparative analysis, we observed that similar to $\Delta ubiI$, $\Delta ubiK$ showed statistically significant fitness defect only in oleate (Dataset S1, FDR <5%; Fig. 1C).

To further strengthen our proposal that reduced levels of ubiquinone are suboptimal for growth in oleate thus leading to oxidative stress, we independently compared ubiquinone levels in $\Delta ubiI$ and $\Delta ubiK$, validated the growth defect of $\Delta ubiK$ in candidate studies and determined ROS levels in $\Delta ubiK$. Q₈ levels were reduced to ~15-20% in both $\Delta ubiI$ and $\Delta ubiK$, and a peak corresponding to an intermediate (elution time: ~15 min) was observed in both the strains (Fig. 5A; Fig. S5). Except oleate, $\Delta ubiK$ did not show growth defect on any other non-fermentable carbon source (Fig. 5B). The growth defect on oleate was complemented by *ubiK* cloned on plasmid (Fig. 5C), concomitant with restoration of ubiquinone levels (Fig. S6). Further, similar to *ubi* deletion strains, compared to WT in TB, ROS levels were ~2.5-fold higher in $\Delta ubiK$ in TB-Ole (Fig. 5D).

The related phenotypes of $\Delta ubiI$ and $\Delta ubiK$ prompted us to examine the phenotype of $\Delta ubiI\Delta ubiK$ double mutant. In contrast to the normal growth of $\Delta ubiI$ and $\Delta ubiK$ in LB medium, the double mutant formed tiny colonies on LB (Fig. 5E). In order to determine ubiquinone levels in the $\Delta ubiI\Delta ubiK$ strain, we resorted to growing the cultures in a rich LB-glucose medium, where there is reduced dependency on ubiquinone for growth (50). Interestingly, there was no detectable ubiquinone in the $\Delta ubiI\Delta ubiK$ double mutant (Fig. 5F; Fig. S7), suggesting redundancy in the ubiquinone biosynthesis pathway. Importantly, similar to single *ubi* deletion strains (*ubiE*, *ubiF* and *ubiH*) that produce no detectable ubiquinone, the $\Delta ubiI\Delta ubiK$ double mutant showed growth defect in glucose but did not grow at all with oleate, acetate and succinate (Fig. 5G). Taken together, our data convincingly establishes that there is a differential requirement of ubiquinone

amongst non-fermentable carbon sources, requirement being maximal in oleate to alleviate oxidative stress.

DISCUSSION

Quantitative contribution of Nuo and Cyo to growth is inversely correlated with the energy yield of non-fermentable carbon sources

The important functions of ETC are ATP production and maintenance of redox balance. We find that Nuo is the major NADH dehydrogenase for aerobic growth on oleate, acetate and succinate (Datasets S1A and C; Fig. 1C and 2). Because *nuo* mutants would be unable to oxidize NADH efficiently this would increase NADH/NAD⁺ ratios, which might further inhibit TCA and glyoxylate cycle enzymes resulting in a decrease in cellular metabolites (28). Besides, since Nuo is a proton pump ($H^+/e^- = 2$) (8), its deletion would lead to decrease in ATP synthesis in the cell. Therefore, in *nuo* mutants grown on non-fermentable carbon sources ATP would be produced mainly from FADH₂ oxidation.

The Δ *nuo* strain exhibited no growth in acetate (Fig. 2). We speculate that in acetate, in addition to increased NADH/NAD⁺ ratio and decrease in cellular metabolites, *nuo* mutant cannot produce energy to support growth because only 1 molecule of ATP will be generated per acetate molecule considering ATP:FADH₂ ratio to be 1 (8). However, 1 molecule of ATP is also expended to activate acetate to acetyl-CoA (4), thus in a *nuo* mutant there will be no net ATP gain. On the other hand *nuo* mutant exhibited extended lag in oleate and succinate (Fig. 2). We suggest that since *nuo* mutant can generate energy from oxidation of FADH₂ produced during β -oxidation of oleate and in the first step of succinate utilization (4,51), this allows cells to re-adjust its metabolism to maintain redox balance resulting in same growth rate and growth yield as WT cells. Further, unlike acetate, activation of succinate is not required for its metabolism and although conversion of oleate to oleoyl-CoA is required for oleate metabolism, only 1 molecule of ATP is consumed per 18 carbon atoms (4,51). Reduced energy generation might also be the reason for the significant growth defect of Δ *cyo* strains in acetate (Fig. 1C). Since Cyo, the major terminal oxidase during aerobic metabolism generates proton motive force ($H^+/e^- = 2$) (8),

disruption of Cyo complex would be expected to result in a more compromised growth on carbon sources such as acetate that have poor net ATP yield.

Ubiquinone relieves oxidative stress generated by LCFAs

It was surprising that unlike other ETC components, requirement of ubiquinone, the electron carrier of ETC, did not correlate with the energy yield of non-fermentable carbon sources. Our detailed analysis shows that ubiquinone was maximally required in oleate to mitigate elevated levels of ROS. Compared to WT cells, ROS levels were ~1.5-fold higher in a Δ *ubiI* strain grown in glucose, acetate or succinate but there was no difference in the growth profile of WT and Δ *ubiI* in these carbon sources (Fig. 3A and D). The utilization of oleate resulted in ~1.5-fold increase in ROS levels in WT cells compared to other carbon sources which further increased to ~2.5-fold in a Δ *ubiI* strain (Fig. 3D). Importantly, this elevated level of ROS (~2.5-fold) was deleterious as evident from the significant growth defect of Δ *ubiI* strain in oleate and that the growth defect could be partially recovered by chemical antioxidants (Fig. 3). These data clearly indicate that in oleate utilizing cells optimum levels of ubiquinone are required to manage ROS below a toxic threshold. Further, we find that amongst various oxidative stress combat players, ubiquinone is the key antioxidant during LCFA metabolism. This is supported by the observation that strains deleted for oxidative stress combat players other than *ubi* genes do not exhibit increase in ROS in oleate-utilizing cells (Fig. 4A). Moreover, whereas ubiquinone accumulates in the presence of oleate, other players are induced only in a mutant defective in ubiquinone biosynthesis (Fig. 4B, C and E). Interestingly, oleate degradation generates ROS and also provides a signal for ubiquinone accumulation (Fig. 4E and F). These results suggest a feedback loop that prevents excessive ROS formation during growth in LCFAs.

An earlier study has shown that ubiquinone is present in excess over flavins and cytochromes in the *E. coli* inner membrane (52). Thus under normal conditions ubiquinone is not limiting for its electron transfer function.

Considering this, ~2-fold increase in ubiquinone levels in cells utilizing oleate could bring a significant physiological response. Few *ubi* genes are regulated by the ArcA-ArcB two-component system and catabolite repression (53-57). It will be interesting to investigate the mechanisms that regulate ubiquinone levels during LCFA degradation. We suggest that ROS itself might not be the signal for upregulation of ubiquinone, since despite exhibiting higher level of ROS Δ *fadD* strain had basal ubiquinone levels in TB medium (compare Fig. 4E and F).

Succinate has been extensively used for screening *ubi* genes (34,35). We suggest that oleate is a better carbon source than succinate for identifying *ubi* players especially ones that have partial effect on ubiquinone levels. The unique requirement of *ubiI* and *ubiK* for growth in oleate validates this suggestion (Fig. 1C, 3A and 5B; Fig. S1). UbiK is a small protein (<100 amino acids) that belongs to BMFP (*Brucella* Membrane Fusogenic Protein) superfamily. In *S. typhimurium*, it is involved in the regulation of flagella and fimbriae expression, motility, colonization and virulence of the organism (29,58,59). *E. coli* UbiK physically interacts with a non-enzymatic ubiquinone biosynthesis player, UbiJ, and is proposed to be an assembly factor for additional Ubi proteins (29). Our results that a double mutant of *ubiK* and an enzyme involved in ubiquinone biosynthesis, *ubiI*, shows synthetic sick/lethal phenotype with no detectable ubiquinone provides a strong genetic evidence of the interaction between UbiK and other Ubi proteins (Fig. 5E, F and G; Fig. S7).

Proposed mechanisms by which ubiquinone might counteract LCFA-mediated oxidative stress

Several mechanisms have been suggested for ROS formation that includes extraction of electrons from reduced metal centers of certain enzymes by molecular O₂, leakage of electrons during oxidation-reduction cycles of ETC promoting the reaction of free electrons with O₂ and auto-oxidation of flavoproteins (14,15,60). Soballe and Poole first demonstrated the role of ubiquinone in counteracting ROS in bacteria and proposed two mechanisms to explain its antioxidant function. First, ubiquinone limits ROS formation due to its ability to rapidly transfer electrons from upstream

respiratory dehydrogenases to terminal oxidases thereby decreasing the chance of single-electron donation to oxygen. Second, the reduced form of ubiquinone (ubiquinol) can scavenge ROS (15).

Fig. 6 shows the probable sites of ROS formation during growth of *E. coli* in LCFAs and the mechanisms by which ubiquinone might counteract LCFA-induced oxidative stress. Regarding the site of ROS formation, we speculate that during LCFA catabolism, high NADH/NAD⁺ and FADH₂/FAD ratios would increase electron flow in the ETC thereby increasing the probability of electron leakage and auto-oxidation of reduced form of respiratory dehydrogenases resulting in elevated levels of ROS. Importantly, a predominant source of ROS during LCFA degradation could be the acyl-CoA dehydrogenase, FadE, which catalyzes the oxidation of acyl-CoA to enoyl-CoA concomitant with reduction of FAD to FADH₂. Whether FadE itself re-oxidizes FADH₂ and directly transfers electrons to ubiquinone or requires the involvement of an electron transfer flavoprotein (ETF) and ETF-quinone oxidoreductase is unclear (61). Nevertheless, the oxidation of reduced flavin bound to FadE could result in ROS formation. Concerning the possible mechanisms by which ubiquinone might combat ROS, our results suggest that its antioxidant role cannot be explained solely by the ability to transfer electrons from NADH and succinate dehydrogenases to terminal oxidases since amongst all these ETC components only ubiquinone was more important on LCFAs when compared to other non-fermentable carbon sources (Fig. 1C, 2, 3A and 5B; Fig. S1). It is likely that ubiquinone also limits ROS formation at FadE by transferring electrons from FadE to the ETC. In addition, a recent study has demonstrated the *in vitro* quinol peroxidase activity of Cyd where quinol serves as a substrate for the peroxidase to detoxify H₂O₂ (62). Thus, during LCFA catabolism, besides decreasing ROS formation owing to its electron shuttling role in ETC, ubiquinone might promote the peroxidase activity of terminal oxidase to detoxify ROS. Since ETC is one of the sites for ROS formation, it might be advantageous for the cell to have antioxidant in the membrane to detoxify ROS locally. Ubiquinone in conjunction with Cyd might fulfill this role.

Several bacterial pathogens use LCFAs derived from host tissues as their nutrient source

(1-3). It will be interesting to examine whether ubiquinone participates in managing LCFA-mediated oxidative stress in these pathogens. In fact *ubiB*, *ubiE*, *ubiJ*, and *ubiK* mutants of *S. typhimurium* are impaired for intracellular proliferation in macrophages (29,63). Since *S. typhimurium* utilizes fatty acids in macrophages during chronic infection (2), it is possible that ubiquinone is required by this intracellular pathogen to combat oxidative stress generated by LCFAs.

EXPERIMENTAL PROCEDURES

Strains and plasmids

Chemical genomics screen used the Keio deletion library derived from BW25113 (16). Majority of the follow-up experiments were conducted in BW25113 background, and either both independent clones from the library and/or fresh transductants were analyzed to rule out genetic errors. Strains, plasmids, and primers used for plasmid construction are listed in Table S1.

Media composition and growth conditions

Media had the following composition: M9 minimal medium- 5.3 g/L Na₂HPO₄, 3 g/L KH₂PO₄, 0.5 g/L NaCl, 1g/L NH₄Cl, 1.2 g/L MgSO₄, 2 mg/L Biotin, 2 mg/L Nicotinamide, 0.2 mg/L Riboflavin, and 2 mg/L Thiamine; Lysogeny Broth (LB)- 5 g/L yeast extract, 10 g/L Bacto Tryptone, and 5 g/L NaCl; and Tryptone Broth (TB)- 10 g/L Bacto Tryptone, and 5 g/L NaCl. Unless otherwise specified, when required, media were supplemented with one of the following carbon sources at a final concentration of 5 mM: glucose or sodium salt of acetate, succinate, or oleate. Stock of oleate (50 mM) was prepared in 5.0% Brij-58 (64). Media were solidified using 1.5% (w/v) bacto agar. For chemical genomics screen, minimal medium was supplemented either with 5 mM oleate or 0.2% glucose with 0.5% Brij-58. To facilitate comparison of our screen on oleate with published screens on other carbon sources (17), same concentration of glucose was used in our control condition.

Cultures were incubated at 37°C. For experiments in liquid medium, unless indicated otherwise, primary cultures were grown in 3 ml TB, which were further re-inoculated either in TB or TB supplemented with desired carbon source to an initial OD₆₀₀ of ~0.01. These secondary cultures

were grown for defined time periods. For the detection of Q₈ in $\Delta ubiI\Delta ubiK$ double mutant, strains were grown in LB supplemented with 0.2% glucose.

Library screening and data processing

The chemical genomics screen was performed using the same methodology as reported previously with slight modifications (17). Briefly, the Keio deletion library was arrayed in 1536-format and pinned onto plates containing minimal medium agar supplemented either with oleate or glucose with Brij-58, using a Singer Rotor robot. Plates were incubated at 37°C for 21 hours for glucose with Brij-58 and 42 hours for oleate. Time points were chosen such that fitness differences were apparent but growth had not saturated.

Pictures of the plates were taken using a Canon G10 digital camera. Colony size was quantified from plate images using the HT Colony Grid Analyzer software package (18). Colony sizes were filtered and normalized using established methods for chemical genomics in *E. coli* K-12 (19). To account for potential effects of Brij-58 on growth, fitness scores for the oleate condition were generated by directly comparing colony size between oleate and glucose with Brij-58 control using the same statistical test as the S-score (18).

To facilitate comparison of the chemical genomic profile of oleate to other carbon sources, raw data from minimal media conditions of a previous large-scale chemical genomic screen (17) were reanalyzed using the same workflow above and M9 minimal with 0.2% glucose as a normalization. Finally, fitness score distributions for each condition were scaled to have a standard inter-quartile range of 1.35 (17) to minimize bias in any downstream analysis from conditions with a large variance. The MATLAB code and raw data for this analysis are available online at https://github.com/AnthonyShiverMicrobes/fitness_lcf.

Growth curves

Overnight cultures grown in LB were pelleted, washed and re-suspended in M9 minimal medium. Cells were re-inoculated in 200 μ l M9 minimal medium containing the desired carbon source to a starting OD₄₅₀ of ~0.03, in 96-well plates, using a robotic liquid handling system (Tecan). When

required, antibiotic, glutathione, thiourea or urea at a desired concentration was added to the medium. Plates were incubated in a shaker at 37°C, and OD₄₅₀ of the cultures was measured at designated time intervals (Tecan Infinite M200 monochromator). The incubator shaker and microplate reader were integrated with the liquid handling system, and the transfer of plates between shaker and reader was automated.

Dilution spotting

Overnight cultures grown in LB were pelleted, washed and re-suspended in M9 minimal medium. Several dilutions of cultures were spotted on M9 minimal medium containing the desired carbon source. Antibiotic was added whenever required. Plates were incubated and imaged at various time intervals using the Gel Doc XR⁺ imaging system from BioRad. A representative image where growth differences were apparent is shown in the figures.

Nitroblue tetrazolium (NBT) reduction assay

Secondary cultures (3 ml) were grown in culture tubes (27 ml capacity) for 16 hours. ROS levels were determined by NBT reduction assay following the protocol described in (42) with slight modifications. Cells were pelleted and washed with Hanks' balanced salt solution (HBSS). Washing was required to remove growth medium to avoid interference of Brij-58. 10⁹ cells were re-suspended in 0.2 ml HBSS and were split in two aliquots: 0.5 ml NBT (1 mg/ml) was added to one aliquot and the other aliquot was left untreated. Both aliquots were incubated at 37°C for 30 min. 0.1 ml of 0.1 M HCl was added and samples were centrifuged at 18,400 X g for 15 min. Supernatant was discarded, and pellet was treated with 0.4 ml dimethyl sulfoxide (DMSO) to dissolve reduced NBT (formazan blue), followed by addition of 0.8 ml HBSS. Formazan blue was quantified at 575 nm. To determine the absorbance corresponding to formazan blue, absorbance of aliquot without NBT was deducted from absorbance obtained for NBT treated sample. For experiments where ROS levels were determined in different phases of growth, 15 ml secondary cultures were grown in 125 ml flasks. Independent cultures (from the same primary culture) were set-up for each time point.

β-galactosidase assay

β-gal assays were performed in MC4100 background. Secondary cultures (15 ml) were grown in 125 ml flasks for 14-16 hours. Cells were pelleted, washed at least 4 times with Z-buffer and diluted to OD₄₅₀ ~0.5. Several washings of the culture were critical to remove Brij-58 since the detergent interferes with β-gal assay. *katG* and *ahpC* promoter activity was measured by monitoring β-gal expression from single-copy *katG-lacZ* and *ahpC-lacZ* transcriptional fusion, respectively as described (65).

Preparation of ubiquinol standard

Ubiquinol-8 was prepared by reduction of ubiquinone-8 (Avantis Polar Lipids) following the procedure used for reduction of ubiquinone-10 (66). Briefly, 19 ml hexane was added to 1 ml ubiquinone solution (1 mg/ml in hexane). 1 ml methanol and 200 mg sodium borohydride were added (solution was covered to avoid light), stirred and kept for 5 min. 2 ml water was added and mixed thoroughly to dissolve sodium borohydride. The mix was centrifuged at 2050 X g for 5 min. Colorless organic supernatant was transferred to a fresh tube and stored at -20°C. The conversion of yellow colored ubiquinone-8 to colorless ubiquinol-8 indicated complete reduction.

Quinone extraction and detection by HPLC-Photodiode Array (PDA) detection analysis

Quinones were extracted using the protocol described in (31) with slight modifications. 15 ml secondary cultures were grown in 125 ml flasks for 16 hours. Equal number of cells (~3 x 10¹⁰ cells) for all cultures were pelleted and the pellet mass was determined. Pellets were re-suspended in 100 μl of 0.15 M KCl and to the re-suspension 200 μl glass beads (acid washed ≤ 106 μm, Sigma), 600 μl methanol and 12 μg ubiquinone-10 standard (Sigma) in hexane (used as internal control for extraction efficiency) were added. Samples were vortexed for 15 min, and 400 μl hexane was added. Samples were again vortexed for 3 min and then centrifuged at 3380 X g for 1 min. Upper hexane layer was transferred to fresh micro-centrifuge tube. 100 μl of this hexane layer was completely dried under vacuum and re-suspended in 100 μl of mobile phase, an isocratic solution constituted by using 40% ethanol, 40% acetonitrile, and 20% of a mix of 90% isopropyl

alcohol and 10% lithium perchlorate (1 M). Lipid extracts were separated by reverse-phase HPLC with a C18 column (Waters Sunfire 5 μ m column, 4.6 X 250 mm) at a flow rate of 1 ml/min using mobile phase. Quinones were detected using a Photodiode array detector. In order to detect total Q₈ (ubiquinone-8 + ubiquinol-8) in samples, λ_{\max} of ubiquinone-8 and ubiquinol-8 standards was determined by scanning from 240 nm to 399 nm. λ_{\max} of ubiquinone-8 was 275 nm, and that of

ubiquinol-8 was 290 nm. Peaks for ubiquinone-8 and ubiquinol-8 in the effluent were assigned based on the elution time of pure standards, and reduction of ubiquinone-8 and ubiquinol-8 peaks in $\Delta ubiI$ strain. For each sample, Q₈ peak area per unit mass was calculated, and to account for difference in extraction efficiency between samples, Q₈ peak area per unit mass was divided by ubiquinone-10 peak area.

ACKNOWLEDGMENTS

We acknowledge Carol Gross for access to the robotics facility for high-throughput genetic screens. We thank Gisela Storz for strains GS022 and MC4100 *ahpC-lacZ*, and plasmid pAQ6, and Frédéric Barras for strain BEFB05. We especially thank Patricia Kiley for valuable suggestions and critical reading of the manuscript. We thank members of the Chaba lab for discussions. SA and TP acknowledge fellowship support from IISER-Mohali for doctoral and postdoctoral work, respectively. KJ and HB are recipients of DST-Inspire fellowship for doctoral and undergraduate studies, respectively. This work was supported by start-up funds from IISER-Mohali to RC and was partly funded by CSIR (project no. 37(1623)/14/EMR-II), Govt. of India to RC.

CONFLICT OF INTEREST

The authors declare that they have no conflict of interest with the contents of this article.

AUTHOR CONTRIBUTIONS

RC, SA, and KJ designed the study. RC performed the high-throughput genetic screen. ALS performed analysis of the high-throughput data. SA, KJ and HB performed follow-up experiments. TP standardized initial experiments. RC, KJ, SA, ALS and HB wrote the manuscript. All authors reviewed and edited the manuscript. RC supervised the project.

REFERENCES

1. McKinney, J. D., Honer zu Bentrup, K., Munoz-Elias, E. J., Miczak, A., Chen, B., Chan, W. T., Swenson, D., Sacchetti, J. C., Jacobs, W. R., Jr., and Russell, D. G. (2000) Persistence of *Mycobacterium tuberculosis* in macrophages and mice requires the glyoxylate shunt enzyme isocitrate lyase. *Nature* **406**, 735-738
2. Fang, F. C., Libby, S. J., Castor, M. E., and Fung, A. M. (2005) Isocitrate lyase (AceA) is required for *Salmonella* persistence but not for acute lethal infection in mice. *Infect Immun* **73**, 2547-2549
3. Son, M. S., Matthews, W. J., Jr., Kang, Y., Nguyen, D. T., and Hoang, T. T. (2007) In vivo evidence of *Pseudomonas aeruginosa* nutrient acquisition and pathogenesis in the lungs of cystic fibrosis patients. *Infect Immun* **75**, 5313-5324
4. Clark, D. P., and Cronan, J. E. (7 October 2005, posting date) Two-carbon compounds and fatty acids as carbon sources. in *EcoSal—Escherichia coli and Salmonella: Cellular and Molecular Biology*. (R. Curtiss III ed.), <http://www.ecosal.org>. ASM Press, Washington, DC. pp

5. Cronan, J. E., and Laporte, D. (9 November 2006, posting date) Tricarboxylic acid cycle and glyoxylate bypass. in *EcoSal—Escherichia coli and Salmonella: Cellular and Molecular Biology*. (R. Curtiss III ed.), <http://www.ecosal.org>. ASM Press, Washington, DC. pp
6. Campbell, J. W., Morgan-Kiss, R. M., and Cronan, J. E., Jr. (2003) A new *Escherichia coli* metabolic competency: growth on fatty acids by a novel anaerobic beta-oxidation pathway. *Mol Microbiol* **47**, 793-805
7. Berger, E. A. (1973) Different mechanisms of energy coupling for the active transport of proline and glutamine in *Escherichia coli*. *Proc Natl Acad Sci U S A* **70**, 1514-1518
8. Unden, G., and Dunnwald, P. (11 March 2008, posting date) The aerobic and anaerobic respiratory chain of *Escherichia coli* and *Salmonella enterica*: enzymes and energetics. in *EcoSal—Escherichia coli and Salmonella: Cellular and Molecular Biology*. (R. Curtiss III ed.), <http://www.ecosal.org>. ASM Press, Washington, DC. pp
9. Aussel, L., Pierrel, F., Loiseau, L., Lombard, M., Fontecave, M., and Barras, F. (2014) Biosynthesis and physiology of coenzyme Q in bacteria. *Biochim Biophys Acta* **1837**, 1004-1011
10. Falk-Krzesinski, H. J., and Wolfe, A. J. (1998) Genetic analysis of the *nuo* locus, which encodes the proton-translocating NADH dehydrogenase in *Escherichia coli*. *J Bacteriol* **180**, 1174-1184
11. Au, D. C., and Gennis, R. B. (1987) Cloning of the *cyo* locus encoding the cytochrome *o* terminal oxidase complex of *Escherichia coli*. *J Bacteriol* **169**, 3237-3242
12. McNeil, M. B., Clulow, J. S., Wilf, N. M., Salmond, G. P., and Fineran, P. C. (2012) SdhE is a conserved protein required for flavinylation of succinate dehydrogenase in bacteria. *J Biol Chem* **287**, 18418-18428
13. Doi, H., Hoshino, Y., Nakase, K., and Usuda, Y. (2014) Reduction of hydrogen peroxide stress derived from fatty acid beta-oxidation improves fatty acid utilization in *Escherichia coli*. *Appl Microbiol Biotechnol* **98**, 629-639
14. Imlay, J. A. (2013) The molecular mechanisms and physiological consequences of oxidative stress: lessons from a model bacterium. *Nat Rev Microbiol* **11**, 443-454
15. Soballe, B., and Poole, R. K. (2000) Ubiquinone limits oxidative stress in *Escherichia coli*. *Microbiology* **146** (Pt 4), 787-796
16. Baba, T., Ara, T., Hasegawa, M., Takai, Y., Okumura, Y., Baba, M., Datsenko, K. A., Tomita, M., Wanner, B. L., and Mori, H. (2006) Construction of *Escherichia coli* K-12 in-frame, single-gene knockout mutants: the Keio collection. *Mol Syst Biol* **2**, 2006 0008
17. Nichols, R. J., Sen, S., Choo, Y. J., Beltrao, P., Zietek, M., Chaba, R., Lee, S., Kazmierczak, K. M., Lee, K. J., Wong, A., Shales, M., Lovett, S., Winkler, M. E., Krogan, N. J., Typas, A., and Gross, C. A. (2011) Phenotypic landscape of a bacterial cell. *Cell* **144**, 143-156
18. Collins, S. R., Schuldiner, M., Krogan, N. J., and Weissman, J. S. (2006) A strategy for extracting and analyzing large-scale quantitative epistatic interaction data. *Genome Biol* **7**, R63

19. Shiver, A. L., Osadnik, H., Kritikos, G., Li, B., Krogan, N., Typas, A., and Gross, C. A. (2016) A chemical-genomic screen of neglected antibiotics reveals illicit transport of kasugamycin and blasticidin S. *PLoS Genet* **12**, e1006124
20. Subramanian, A., Tamayo, P., Mootha, V. K., Mukherjee, S., Ebert, B. L., Gillette, M. A., Paulovich, A., Pomeroy, S. L., Golub, T. R., Lander, E. S., and Mesirov, J. P. (2005) Gene set enrichment analysis: a knowledge-based approach for interpreting genome-wide expression profiles. *Proc Natl Acad Sci U S A* **102**, 15545-15550
21. Mootha, V. K., Lindgren, C. M., Eriksson, K. F., Subramanian, A., Sihag, S., Lehar, J., Puigserver, P., Carlsson, E., Ridderstrale, M., Laurila, E., Houstis, N., Daly, M. J., Patterson, N., Mesirov, J. P., Golub, T. R., Tamayo, P., Spiegelman, B., Lander, E. S., Hirschhorn, J. N., Altshuler, D., and Groop, L. C. (2003) PGC-1 α -responsive genes involved in oxidative phosphorylation are coordinately downregulated in human diabetes. *Nat Genet* **34**, 267-273
22. Keseler, I. M., Mackie, A., Peralta-Gil, M., Santos-Zavaleta, A., Gama-Castro, S., Bonavides-Martinez, C., Fulcher, C., Huerta, A. M., Kothari, A., Krummenacker, M., Latendresse, M., Muniz-Rascado, L., Ong, Q., Paley, S., Schroder, I., Shearer, A. G., Subhraveti, P., Travers, M., Weerasinghe, D., Weiss, V., Collado-Vides, J., Gunsalus, R. P., Paulsen, I., and Karp, P. D. (2013) EcoCyc: fusing model organism databases with systems biology. *Nucleic Acids Res* **41**, D605-612
23. Booth, I. R. (29 March 2005, posting date) Glycerol and Methylglyoxal Metabolism. in *EcoSal—Escherichia coli and Salmonella: Cellular and Molecular Biology*. (R. Curtiss III ed.), <http://www.ecosal.org>. ASM Press, Washington, DC. pp
24. Dharmadi, Y., Murarka, A., and Gonzalez, R. (2006) Anaerobic fermentation of glycerol by *Escherichia coli*: a new platform for metabolic engineering. *Biotechnol Bioeng* **94**, 821-829
25. Pipe, L. Z., and Grimson, M. J. (2008) Spatial-temporal modelling of bacterial colony growth on solid media. *Mol Biosyst* **4**, 192-198
26. Friedrich, T., and Pohl, T. (13 August 2007, posting date) NADH as donor. in *EcoSal—Escherichia coli and Salmonella: Cellular and Molecular Biology*. (R. Curtiss III ed.), <http://www.ecosal.org>. ASM Press, Washington, DC. pp
27. Tran, Q. H., Bongaerts, J., Vlad, D., and Udden, G. (1997) Requirement for the proton-pumping NADH dehydrogenase I of *Escherichia coli* in respiration of NADH to fumarate and its bioenergetic implications. *Eur J Biochem* **244**, 155-160
28. Pruss, B. M., Nelms, J. M., Park, C., and Wolfe, A. J. (1994) Mutations in NADH:ubiquinone oxidoreductase of *Escherichia coli* affect growth on mixed amino acids. *J Bacteriol* **176**, 2143-2150
29. Loiseau, L., Fyfe, C., Aussel, L., Hajj Chehade, M., Hernandez, S. B., Faivre, B., Hamdane, D., Mellot-Draznieks, C., Rascalou, B., Pelosi, L., Velours, C., Cornu, D., Lombard, M., Casadesus, J., Pierrel, F., Fontecave, M., and Barras, F. (2017) The UbiK protein is an accessory factor necessary for bacterial ubiquinone (UQ) biosynthesis and forms a complex with the UQ biogenesis factor UbiJ. *J Biol Chem*

30. Pelosi, L., Ducluzeau, A. L., Loiseau, L., Barras, F., Schneider, D., Junier, I., and Pierrel, F. (2016) Evolution of ubiquinone biosynthesis: multiple proteobacterial enzymes with various regioselectives to catalyze three contiguous aromatic hydroxylation reactions. *MSystems* **1**, e00091-00016
31. Hajj Chehade, M., Loiseau, L., Lombard, M., Pecqueur, L., Ismail, A., Smadja, M., Golinelli-Pimpaneau, B., Mellot-Draznieks, C., Hamelin, O., Aussel, L., Kieffer-Jaquinod, S., Labessan, N., Barras, F., Fontecave, M., and Pierrel, F. (2013) *ubiI*, a new gene in *Escherichia coli* coenzyme Q biosynthesis, is involved in aerobic C5-hydroxylation. *J Biol Chem* **288**, 20085-20092
32. Lee, P. T., Hsu, A. Y., Ha, H. T., and Clarke, C. F. (1997) A C-methyltransferase involved in both ubiquinone and menaquinone biosynthesis: isolation and identification of the *Escherichia coli ubiE* gene. *J Bacteriol* **179**, 1748-1754
33. Gulmezian, M., Hyman, K. R., Marbois, B. N., Clarke, C. F., and Javor, G. T. (2007) The role of UbiX in *Escherichia coli* coenzyme Q biosynthesis. *Arch Biochem Biophys* **467**, 144-153
34. Stroobant, P., Young, I. G., and Gibson, F. (1972) Mutants of *Escherichia coli* K-12 blocked in the final reaction of ubiquinone biosynthesis: characterization and genetic analysis. *J Bacteriol* **109**, 134-139
35. Wu, G., Williams, H. D., Gibson, F., and Poole, R. K. (1993) Mutants of *Escherichia coli* affected in respiration: the cloning and nucleotide sequence of *ubiA*, encoding the membrane-bound p-hydroxybenzoate:octaprenyltransferase. *J Gen Microbiol* **139**, 1795-1805
36. Sharma, P., Stagge, S., Bekker, M., Bettenbrock, K., and Hellingwerf, K. J. (2013) Kinase activity of ArcB from *Escherichia coli* is subject to regulation by both ubiquinone and demethylmenaquinone. *PLoS One* **8**, e75412
37. Dwyer, D. J., Belenky, P. A., Yang, J. H., MacDonald, I. C., Martell, J. D., Takahashi, N., Chan, C. T., Lobritz, M. A., Braff, D., Schwarz, E. G., Ye, J. D., Pati, M., Vercruyssen, M., Ralifo, P. S., Allison, K. R., Khalil, A. S., Ting, A. Y., Walker, G. C., and Collins, J. J. (2014) Antibiotics induce redox-related physiological alterations as part of their lethality. *Proc Natl Acad Sci U S A* **111**, E2100-2109
38. Goswami, M., Mangoli, S. H., and Jawali, N. (2006) Involvement of reactive oxygen species in the action of ciprofloxacin against *Escherichia coli*. *Antimicrob Agents Chemother* **50**, 949-954
39. Erental, A., Kalderon, Z., Saada, A., Smith, Y., and Engelberg-Kulka, H. (2014) Apoptosis-like death, an extreme SOS response in *Escherichia coli*. *MBio* **5**, e01426-01414
40. Berridge, M. V., Herst, P. M., and Tan, A. S. (2005) Tetrazolium dyes as tools in cell biology: new insights into their cellular reduction. *Biotechnol Annu Rev* **11**, 127-152
41. Perez-Pantoja, D., Nikel, P. I., Chavarria, M., and de Lorenzo, V. (2013) Endogenous stress caused by faulty oxidation reactions fosters evolution of 2,4-dinitrotoluene-degrading bacteria. *PLoS Genet* **9**, e1003764
42. Albesa, I., Becerra, M. C., Battan, P. C., and Paez, P. L. (2004) Oxidative stress involved in the antibacterial action of different antibiotics. *Biochem Biophys Res Commun* **317**, 605-609

43. Marathe, S. A., Kumar, R., Ajitkumar, P., Nagaraja, V., and Chakravorty, D. (2013) Curcumin reduces the antimicrobial activity of ciprofloxacin against *Salmonella typhimurium* and *Salmonella typhi*. *J Antimicrob Chemother* **68**, 139-152
44. Zhao, H., Kalivendi, S., Zhang, H., Joseph, J., Nithipatikom, K., Vasquez-Vivar, J., and Kalyanaraman, B. (2003) Superoxide reacts with hydroethidine but forms a fluorescent product that is distinctly different from ethidium: potential implications in intracellular fluorescence detection of superoxide. *Free Radic Biol Med* **34**, 1359-1368
45. Petit-Koskas, E., and Contesse, G. (1976) Stimulation in trans of synthesis of *E. coli gal* operon enzymes by lambdaoid phages during low catabolite repression. *Mol Gen Genet* **143**, 203-209
46. Clark, D. (1981) Regulation of fatty acid degradation in *Escherichia coli*: analysis by operon fusion. *J Bacteriol* **148**, 521-526
47. Feng, Y., and Cronan, J. E. (2012) Crosstalk of *Escherichia coli* FadR with global regulators in expression of fatty acid transport genes. *PLoS One* **7**, e46275
48. Pech-Canul, A., Nogales, J., Miranda-Molina, A., Alvarez, L., Geiger, O., Soto, M. J., and Lopez-Lara, I. M. (2011) FadD is required for utilization of endogenous fatty acids released from membrane lipids. *J Bacteriol* **193**, 6295-6304
49. Pradenas, G. A., Paillavil, B. A., Reyes-Cerpa, S., Perez-Donoso, J. M., and Vasquez, C. C. (2012) Reduction of the monounsaturated fatty acid content of *Escherichia coli* results in increased resistance to oxidative damage. *Microbiology* **158**, 1279-1283
50. Zhu, J., Sanchez, A., Bennett, G. N., and San, K. Y. (2011) Manipulating respiratory levels in *Escherichia coli* for aerobic formation of reduced chemical products. *Metab Eng* **13**, 704-712
51. Uden, G., and Kleefeld, A. (30 July 2004, posting date) C4-dicarboxylate degradation in aerobic and anaerobic growth. in *EcoSal—Escherichia coli and Salmonella: Cellular and Molecular Biology*. (R. Curtiss III ed.), <http://www.ecosal.org>. ASM Press, Washington, DC. pp
52. Cox, G. B., Newton, N. A., Gibson, F., Snoswell, A. M., and Hamilton, J. A. (1970) The function of ubiquinone in *Escherichia coli*. *Biochem J* **117**, 551-562
53. Gibert, I., Llagostera, M., and Barbe, J. (1988) Regulation of *ubiG* gene expression in *Escherichia coli*. *J Bacteriol* **170**, 1346-1349
54. Soballe, B., and Poole, R. K. (1997) Aerobic and anaerobic regulation of the *ubiCA* operon, encoding enzymes for the first two committed steps of ubiquinone biosynthesis in *Escherichia coli*. *FEBS Lett* **414**, 373-376
55. Kwon, O., Druce-Hoffman, M., and Meganathan, R. (2005) Regulation of the ubiquinone (coenzyme Q) biosynthetic genes *ubiCA* in *Escherichia coli*. *Curr Microbiol* **50**, 180-189
56. Shimada, T., Fujita, N., Yamamoto, K., and Ishihama, A. (2011) Novel roles of cAMP receptor protein (CRP) in regulation of transport and metabolism of carbon sources. *PLoS One* **6**, e20081
57. Zhang, H., and Javor, G. T. (2003) Regulation of the isofunctional genes *ubiD* and *ubiX* of the ubiquinone biosynthetic pathway of *Escherichia coli*. *FEMS Microbiol Lett* **223**, 67-72

58. Carrica, M. C., Craig, P. O., Garcia-Angulo, V. A., Aguirre, A., Garcia-Vescovi, E., Goldbaum, F. A., and Cravero, S. L. (2011) YqiC of *Salmonella enterica* serovar Typhimurium is a membrane fusogenic protein required for mice colonization. *BMC Microbiol* **11**, 95
59. Wang, K. C., Huang, C. H., Ding, S. M., Chen, C. K., Fang, H. W., Huang, M. T., and Fang, S. B. (2016) Role of *yqiC* in the pathogenicity of *Salmonella* and innate immune responses of human intestinal epithelium. *Front Microbiol* **7**, 1614
60. Imlay, J. A. (2003) Pathways of oxidative damage. *Annu Rev Microbiol* **57**, 395-418
61. Campbell, J. W., and Cronan, J. E., Jr. (2002) The enigmatic *Escherichia coli fadE* gene is *yafH*. *J Bacteriol* **184**, 3759-3764
62. Al-Attar, S., Yu, Y., Pinkse, M., Hoeser, J., Friedrich, T., Bald, D., and de Vries, S. (2016) Cytochrome *bd* displays significant quinol peroxidase activity. *Sci Rep* **6**, 27631
63. Aussel, L., Loiseau, L., Hajj Chehade, M., Pocachard, B., Fontecave, M., Pierrel, F., and Barras, F. (2014) *ubiJ*, a new gene required for aerobic growth and proliferation in macrophage, is involved in coenzyme Q biosynthesis in *Escherichia coli* and *Salmonella enterica* serovar Typhimurium. *J Bacteriol* **196**, 70-79
64. Lepore, B. W., Indic, M., Pham, H., Hearn, E. M., Patel, D. R., and van den Berg, B. (2011) Ligand-gated diffusion across the bacterial outer membrane. *Proc Natl Acad Sci U S A* **108**, 10121-10126
65. Miller, J. H. (1972) *Experiments in molecular genetics* Cold Spring Harbor Laboratory, NY
66. Kotnik D, J.-K. P., Krizman M, Zibert T, Prosek M & Smidovnik A. (2013) Rapid and sensitive HPLC-MS/MS method for quantitative determination of CoQ10. *Research on Precision Instrument and Machinery* **2**, 6-13

FOOTNOTES

†Present address: Department of Signal Transduction and Biogenic Amines, Chittaranjan National Cancer Institute, Kolkata, West Bengal 700026, India.

ABBREVIATIONS

LCFAs, long chain fatty acids; ETC, electron transport chain; ROS, reactive oxygen species; *fad*, fatty acid degradation; TCA, tricarboxylic acid; GSEA, gene set enrichment analysis; TB, tryptone broth; NBT, nitroblue tetrazolium

FIGURE LEGENDS

FIGURE 1. Growth of the Keio deletion library on oleate reveals pathways and ETC components critical for the utilization of LCFAs. (A) Colony sizes of individual mutants are normalized to the plate average and biological replicates (n>3) are plotted for the two conditions tested: oleate and glucose with Brij-58. Points are colored by the logarithm of local density in the plot. Normalized colony sizes from biological replicates are highly correlated (R=0.86, Pearson's correlation). (B) A schematic of the metabolic route of LCFAs highlighting pathways and complexes significantly enriched in oleate. p- and q- represent nominal p-value and FDR q-value, respectively, obtained from GSEA analysis of pathways and complexes in *E. coli*. *FadE is a flavoprotein that reduces FAD to FADH₂ during β-oxidation. It has been speculated that FadE itself might oxidize FADH₂ to FAD by transferring electrons from its dehydrogenase domain to the ETC (61). However, there is no experimental evidence for the same. (C)

Fitness-scores were calculated for oleate and other carbon sources as compared to glucose control. Fitness-scores of components of the β -oxidation pathway and ETC are shown.

FIGURE 2. Amongst NADH dehydrogenases, only Nuo complex is required for growth on non-fermentable carbon sources. WT, Δnuo and Δndh strains were grown in minimal medium containing one of the carbon sources, and OD₄₅₀ was measured. Each medium condition had Brij-58. The experiment was done 4 times; each experiment had 2 technical replicates. A representative dataset with average and SD of technical replicates is shown.

FIGURE 3. The increased requirement of ubiquinone for growth in oleate is to mitigate elevated levels of ROS. (A) $\Delta ubiI$ shows significant growth defect in liquid medium containing oleate as the sole carbon source. WT, $\Delta ubiH$ and $\Delta ubiI$ strains were grown in minimal medium containing one of the carbon sources, and OD₄₅₀ was measured. Each medium condition had Brij-58. (B) and (C) The growth defect of $\Delta ubiI$ in oleate is partially recovered by glutathione (B) and thiourea (C). WT and $\Delta ubiI$ were grown in minimal medium containing oleate with or without 1mM glutathione (GSH) or 1mM thiourea, and OD₄₅₀ was measured. 1mM urea was included as control for thiourea. For Figs 3A, B and C experiments were done 3 times; each experiment had 3 technical replicates. A representative dataset, with average and SD of technical replicates, is shown. (D) WT and $\Delta ubiI$ strains exhibit maximum ROS levels in TB-Ole. WT and $\Delta ubiI$ were grown either in TB or TB supplemented with carbon sources or Brij-58: glucose (TB-Glu), acetate (TB-Ace), succinate (TB-Suc), oleate (TB-Ole), and Brij-58 (TB-Brij). ROS levels were determined by NBT assay. Data were normalized to the ROS level of WT in TB and represent average (\pm SD) of 5 independent experiments. (E) Supplementation of ubiquinone-8 suppresses ROS levels. WT and $\Delta ubiI$ were grown either in TB or TB-Ole. Media contained either 20 μ M ubiquinone-8 or 0.1% ethanol (solvent for ubiquinone-8). ROS levels were determined by NBT assay. Data were normalized to the ROS level of WT in TB containing 0.1% ethanol and represent average (\pm SD) of 3 independent experiments. *P<0.05, **P<0.005 and NS: not significant (unpaired two-tailed Student's t-test).

FIGURE 4. Ubiquinone is a major player that counteracts oxidative stress generated by oleate degradation. (A) In the presence of oleate, ROS levels increase only in strains defective in ubiquinone biosynthesis. WT and various deletion strains were grown either in TB or TB-Ole. ROS levels were determined by NBT assay. Data were normalized to the ROS level of WT in TB and represent average (\pm SD) of 3 independent experiments. (B) and (C) Enzymatic scavengers are induced by oleate when ubiquinone levels are low. WT, $\Delta ubiI$, and $\Delta fadL\Delta ubiI$ strains carrying either *katG-lacZ* (B) or *ahpC-lacZ* (C) (*lacZ* placed under the control of H₂O₂ responsive *katG* or *ahpC* promoter) in MC4100 background, were grown in TB, TB-Brij or TB-Ole, and β -gal activity was determined. Data were normalized to the β -gal activity of WT in TB and represent average (\pm SD) of at least 4 independent experiments. The average β -gal activity of WT carrying *katG-lacZ* in TB was 166 \pm 45 Miller units, and that of WT carrying *ahpC-lacZ* in TB was 38 \pm 15 Miller units. (D) Supplementation of ubiquinone-8 suppresses the induction of *katG-lacZ* in $\Delta ubiI$ grown in TB-Ole. WT and $\Delta ubiI$ strains carrying *katG-lacZ* fusion in MC4100 background were grown either in TB-Brij or TB-Ole. Media contained either 20 μ M ubiquinone-8 or 0.1% ethanol. β -gal activity was determined. Data were normalized to the β -gal activity of WT in TB-Brij with 0.1% ethanol and represent average (\pm SD) of 3 independent experiments. The average β -gal activity of WT in TB-Brij with 0.1% ethanol across 3 experiments was 257 \pm 88 Miller units. **P=0.0058 and NS: not significant (unpaired two-tailed Student's t-test). (E) Ubiquinone accumulates in WT cells in response to oleate utilization. Total Q₈ level in lipid extracts from WT and various *fad* deletion strains grown either in TB or TB-Ole was determined. Q₈ levels were normalized to the Q₈ level of WT in TB and represent average (\pm SD) of at least 4 independent experiments. (F) Oleate transport and degradation is responsible for increase in ROS levels in WT grown in TB-Ole. WT and various *fad* deletion strains

were grown either in TB or TB-Ole. ROS levels were determined by NBT assay. Data were normalized to the ROS level of WT in TB and represent average (\pm SD) of 3 independent experiments.

FIGURE 5. $\Delta ubi\Delta ubiK$ double mutant produces no detectable ubiquinone. (A) $\Delta ubiI$ and $\Delta ubiK$ have similar Q_8 content. Total Q_8 level in lipid extracts from WT, $\Delta ubiI$ and $\Delta ubiK$ cells grown in TB was determined. Q_8 levels were normalized to the Q_8 level of WT in TB and represent average (\pm SD) of 3 independent experiments. (B) $\Delta ubiK$ shows significant growth defect in oleate. Dilutions of the cultures were spotted on minimal medium containing one of the carbon sources. Each medium condition had Brij-58. $\Delta fadL$ was used as a control. The experiment was repeated 3 times. A representative dataset is shown. (C) $ubiK$ cloned on plasmid complements the growth defect of $\Delta ubiK$ in oleate. Dilutions of WT and $\Delta ubiK$ carrying either empty plasmid (pACYC184) or pACYC184 with $ubiK$ (pSA4) were spotted on minimal medium containing oleate as the sole carbon source. $\Delta fadL$ transformed with pACYC184 was used as a control. The experiment was repeated 2 times. A representative dataset is shown. (D) $\Delta ubiK$ strain has increased ROS levels. WT and $\Delta ubiK$ were grown either in TB or TB-Ole, and ROS levels were determined by NBT assay. Data were normalized to the ROS level of WT in TB and represent average (\pm SD) of 3 independent experiments. (E) $\Delta ubiI\Delta ubiK$ shows a synthetically sick phenotype in LB. WT, $\Delta ubiI$, $\Delta ubiK$ and $\Delta ubiI\Delta ubiK$ strains were streaked on LB and incubated overnight. (F) Ubiquinone is not detected in the $\Delta ubiI\Delta ubiK$ double mutant. Total Q_8 level in lipid extracts from WT, $\Delta ubiI$, $\Delta ubiK$ and $\Delta ubiI\Delta ubiK$ cells grown in LB-Glucose was determined. Q_8 levels were normalized to the Q_8 level of WT in LB-Glucose and represent average (\pm SD) of 3 independent experiments. (G) $\Delta ubiI\Delta ubiK$ shows a synthetic lethal phenotype in non-fermentable carbon sources. Dilutions of the cultures were spotted on minimal medium containing one of the carbon sources. Each medium condition had Brij-58. $\Delta fadL$ was used as a control. The experiment was repeated 2 times. A representative dataset is shown.

FIGURE 6. Probable sites of ROS formation during LCFA degradation and the mechanisms employed by ubiquinone to mitigate LCFA-induced oxidative stress. Exogenous LCFAs are transported inside the cell by an outer-membrane protein, FadL. Subsequently, the inner-membrane associated acyl-CoA synthetase, FadD, extracts LCFAs from the inner-membrane concomitant with esterification to acyl-CoA. Acyl-CoAs are degraded to acetyl-CoA via β -oxidation pathway mediated by enzymatic activities of FadE, FadB and FadA. Acetyl-CoA feeds into the TCA cycle for further metabolism. High NADH/NAD⁺ and FADH₂/FAD ratios during β -oxidation and TCA cycle increase electron flow in the ETC thereby increasing electron leakage and auto-oxidation of reduced form of NADH dehydrogenase resulting in ROS formation. In addition, a predominant source of ROS could be the acyl-CoA dehydrogenase, FadE, which reduces FAD to FADH₂. Ubiquinone limits ROS formation by rapidly transferring electrons from upstream dehydrogenases to terminal oxidases (Cyo and Cyd) thus preventing electron leakage and auto-oxidation of reduced form of dehydrogenases. In addition, the quinol peroxidase activity of Cyd will detoxify H₂O₂. Arrows with e⁻ labeled on the line show the direction of electron transfer. Dotted arrows indicate reactions for which either the components involved are not known (oxidation of FadE and electron transfer from FadE to the ETC) or the mechanisms are not established *in vivo* (detoxification of H₂O₂ by Cyd). Abbreviations: LCFA, long chain fatty acid; TCA, tricarboxylic acid; Oaa, oxaloacetate; Cit, citrate; Isocit, isocitrate; α -KG, α -ketoglutarate; Suc-CoA, succinyl-CoA; Suc, succinate; Fum, fumarate; Mal, malate; Glo, Glyoxylate; O₂⁻, superoxide; Sdh, succinate dehydrogenase; Q₈, ubiquinone-8; Q₈H₂, ubiquinol-8; Cyd, cytochrome *bd*; Cyo, cytochrome *bo*.

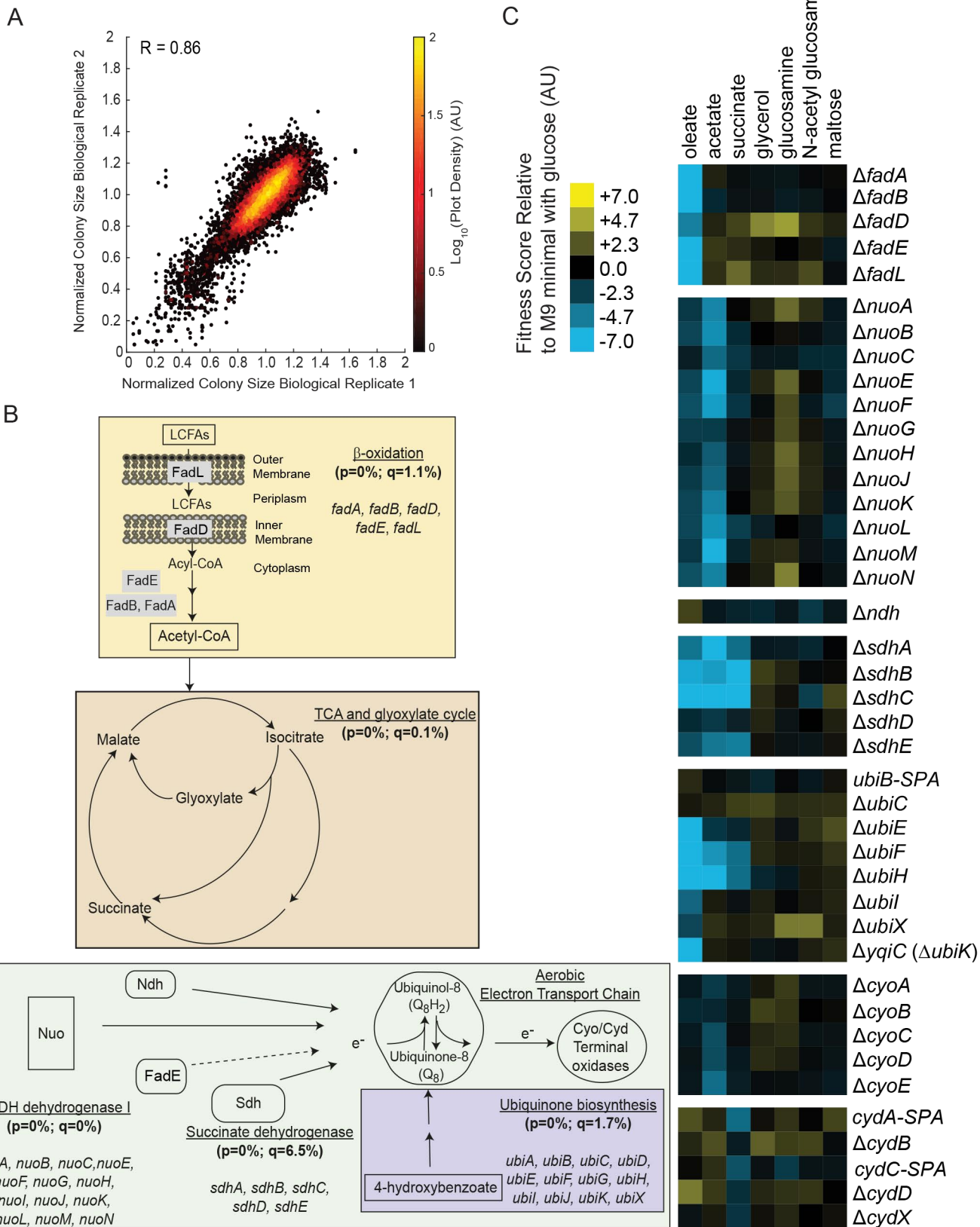


FIGURE 1

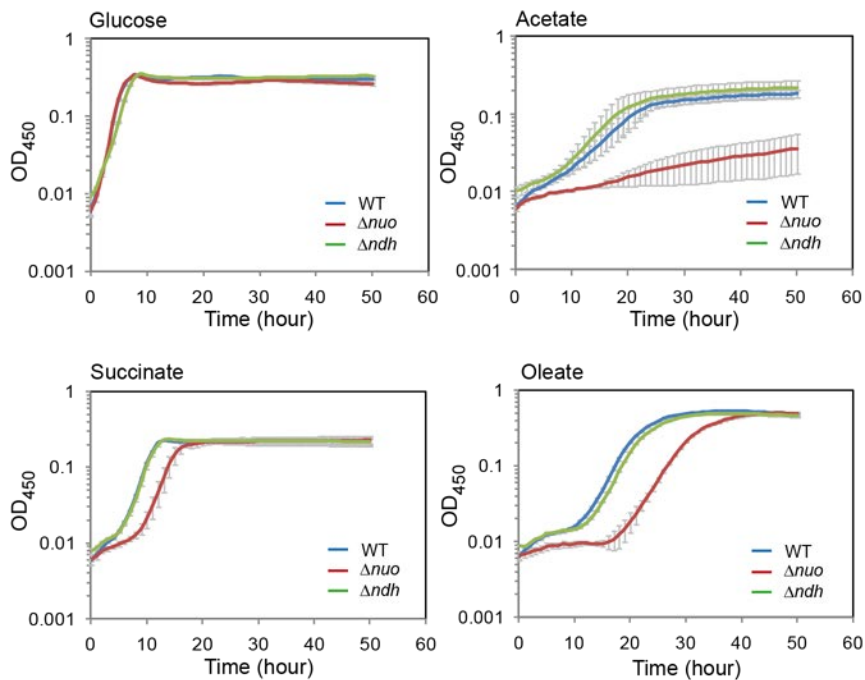


FIGURE 2

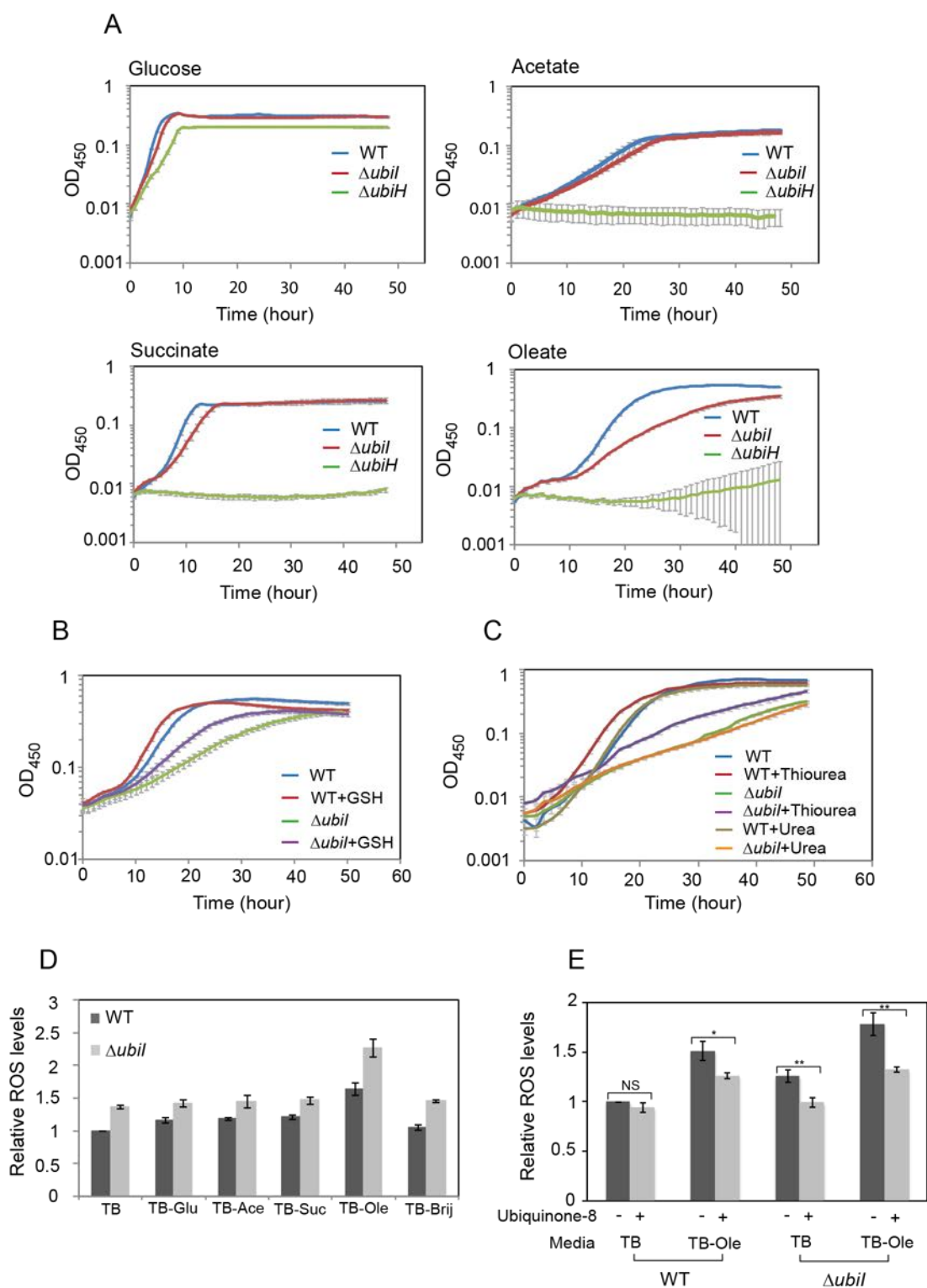


FIGURE 3

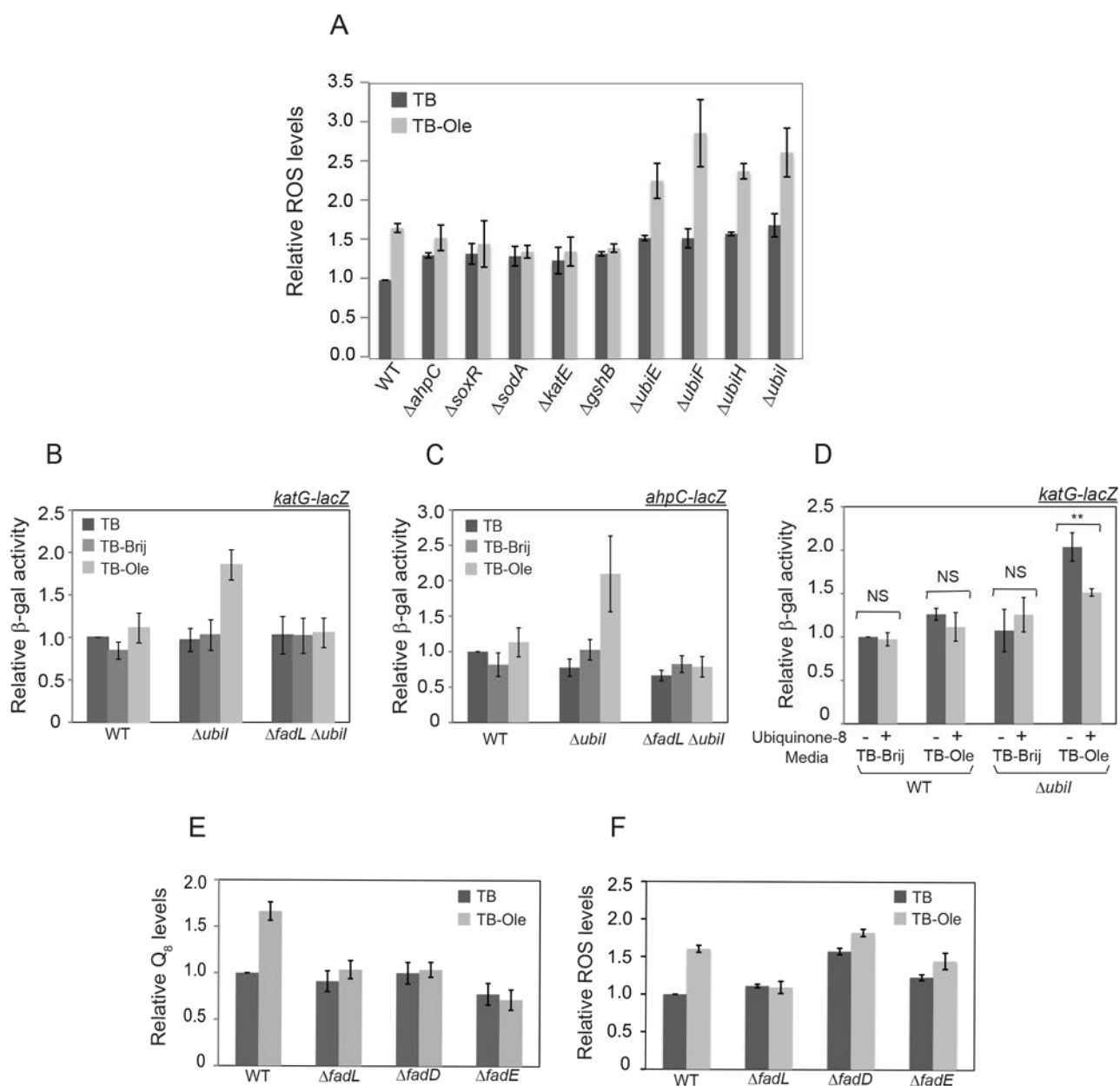


FIGURE 4

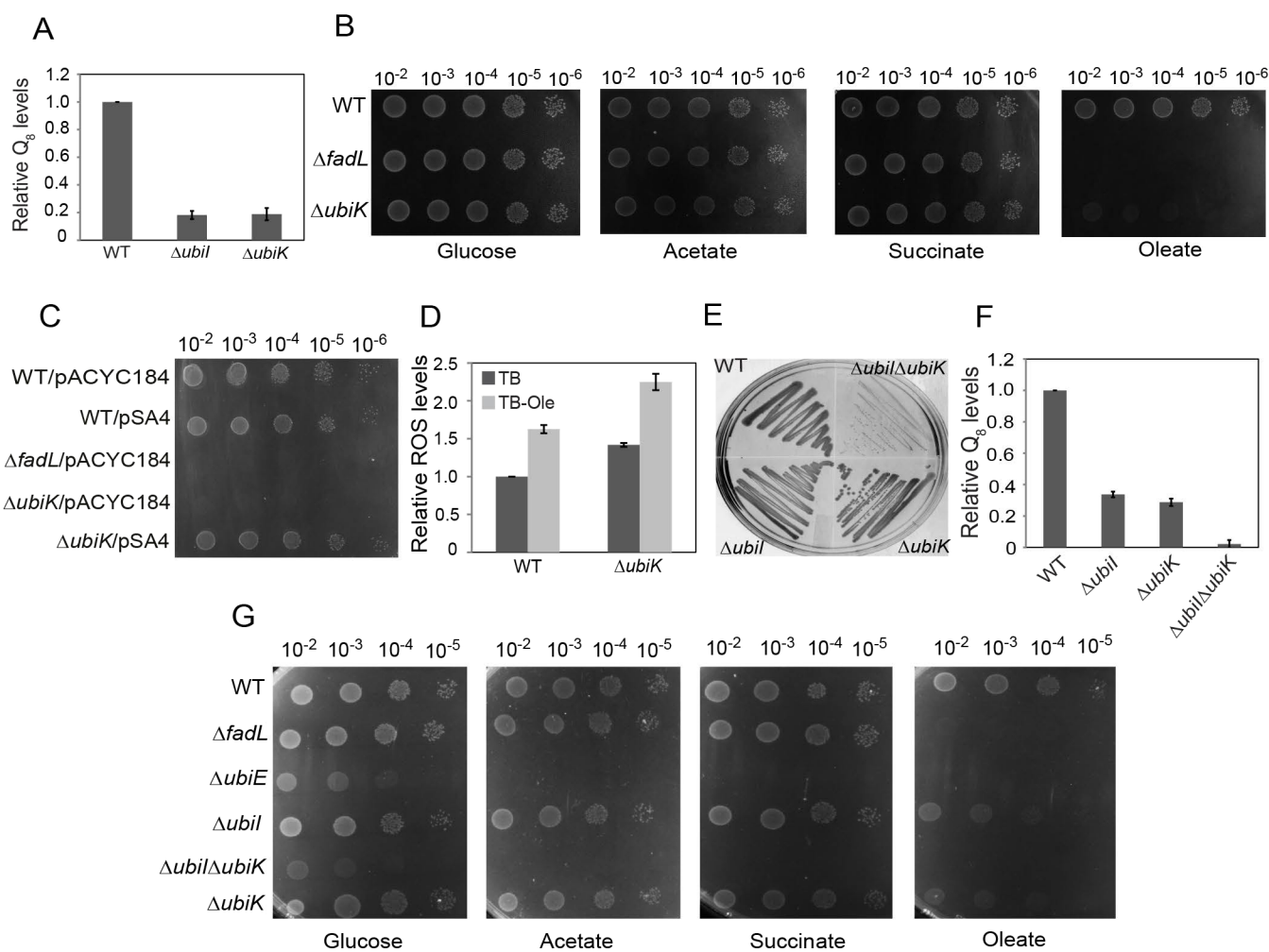


FIGURE 5

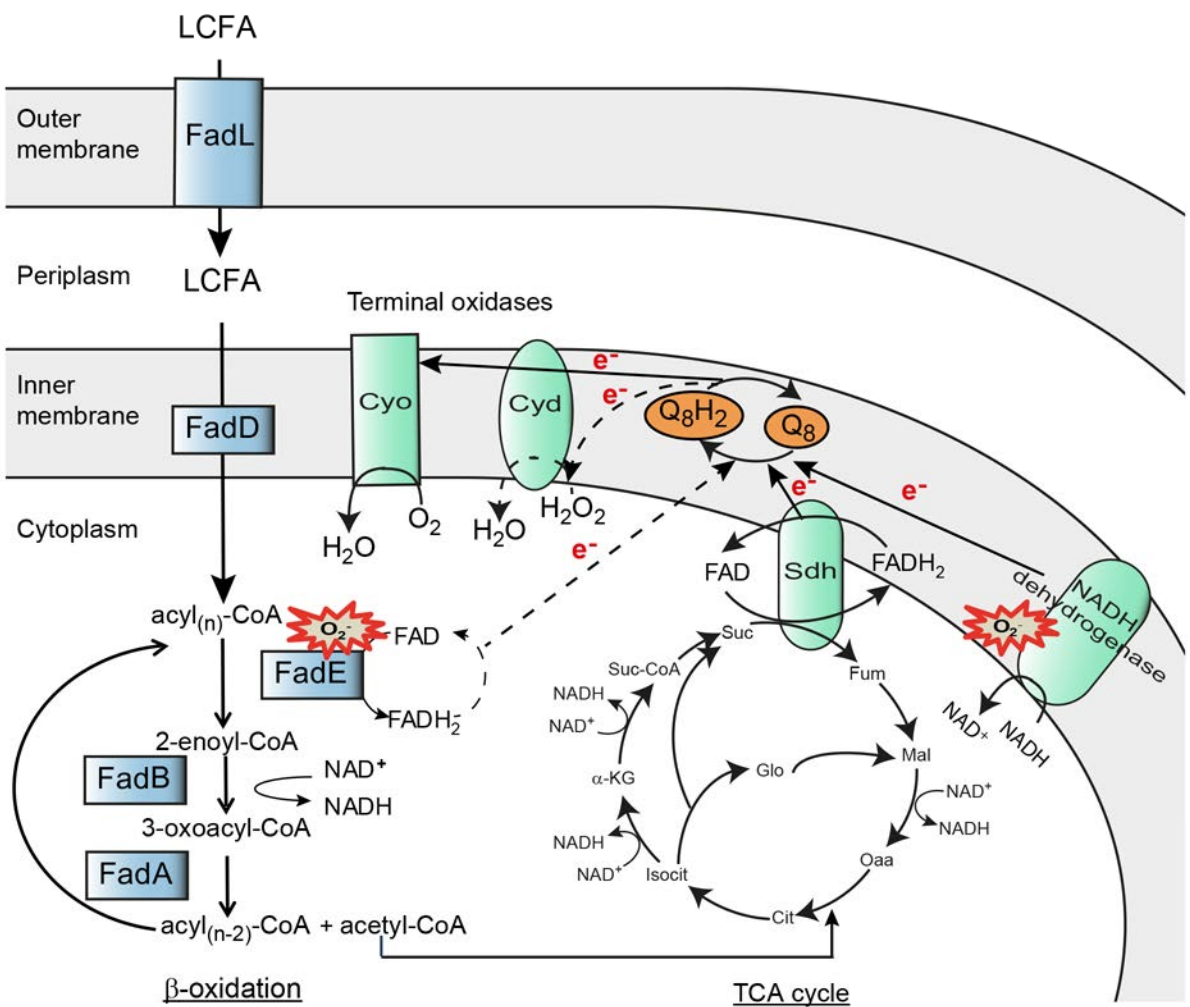


FIGURE 6

A genome-wide screen in *Escherichia coli* reveals that ubiquinone is a key antioxidant for metabolism of long chain fatty acids

Shashank Agrawal, Kanchan Jaswal, Anthony L. Shiver, Himanshi Balecha, Tapas Patra and Rachna Chaba

J. Biol. Chem. published online October 17, 2017

Access the most updated version of this article at doi: [10.1074/jbc.M117.806240](https://doi.org/10.1074/jbc.M117.806240)

Alerts:

- [When this article is cited](#)
- [When a correction for this article is posted](#)

[Click here](#) to choose from all of JBC's e-mail alerts

Supplemental material:

<http://www.jbc.org/content/suppl/2017/10/17/M117.806240.DC1>

This article cites 0 references, 0 of which can be accessed free at

<http://www.jbc.org/content/early/2017/10/17/jbc.M117.806240.full.html#ref-list-1>